

## Supplementary information

### **Tunable Synaptic Plasticity in MoS<sub>2</sub> Neuromorphic Transistor Using Li<sup>+</sup> Incorporated Chitosan Electrolyte**

Lemei Zhu<sup>a</sup>, Chaoqi Dai<sup>a</sup>, Sikai Chen<sup>a</sup>, Airong Liu<sup>a</sup>, Runze Zhan<sup>a</sup>,  
Fangfei Ming<sup>a\*</sup>, Shaozhi Deng<sup>a\*</sup>

<sup>a</sup> *State Key Laboratory of Optoelectronic Materials and Technologies, School of Electronics and Information Technology and Guangdong Province Key Laboratory of Display Material, Sun Yat-sen University, Guangzhou 510275, China*

\* Corresponding author: mingff@mail.sysu.edu.cn; stsdz@mail.sysu.edu.cn

**Supplementary Information:**

Supplementary Figure S1. XPS characterization of the 5 wt%-Li<sup>+</sup>-chitosan film.

Supplementary Figure S2. Experimental impedance diagrams of solid electrolyte films.

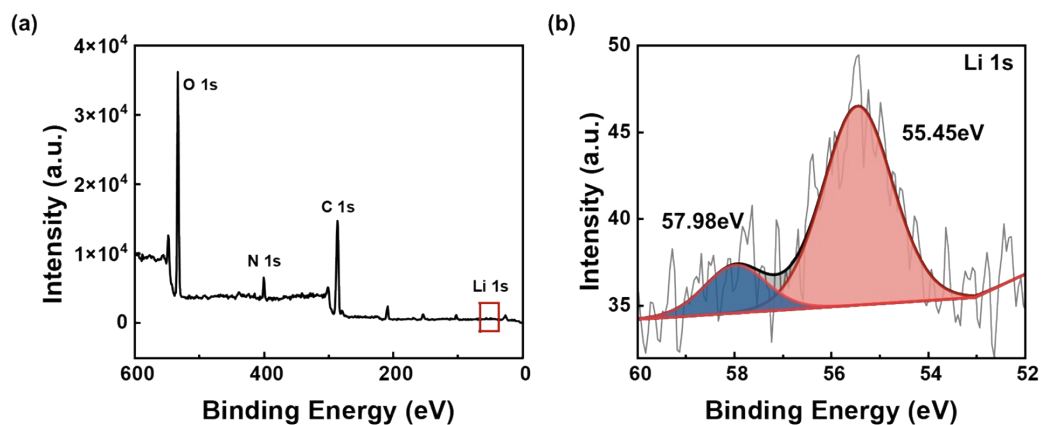
Supplementary Figure S3. Output and transfer characteristics of chitosan and 1 wt%-Li<sup>+</sup>-chitosan EDL-Ts.

Supplementary Figure S4. Gate leakage current characterization.

Supplementary Figure S5. Electrical stability of the 5 wt%-Li<sup>+</sup>-chitosan EDL-T before and after electrolyte cleaning.

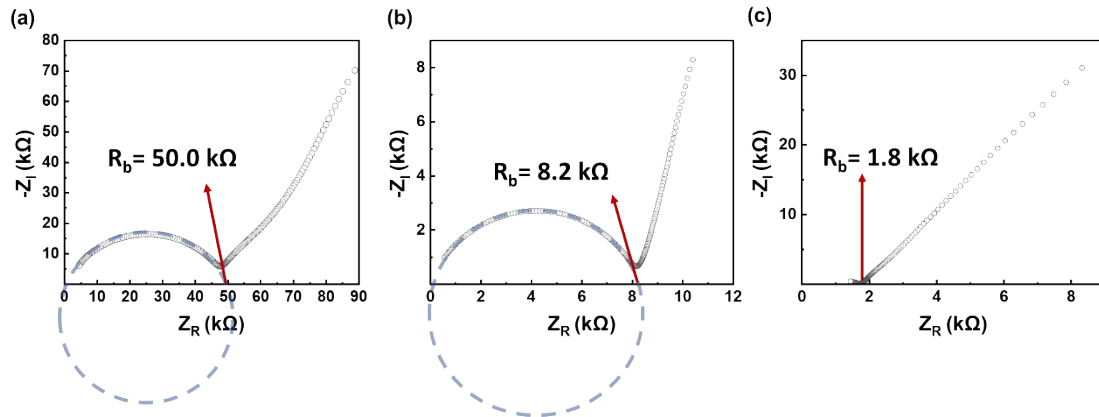
Supplementary Figure S6. Comparison of synaptic responses between a chitosan EDL-T and a 5 wt%-Li<sup>+</sup>-chitosan EDL-T.

Supplementary Figure S7. Stability Test of Chitosan EDL-T and 5 wt% Li<sup>+</sup>-Chitosan EDL-T Devices.



**Supplementary Figure S1. XPS characterization of the 5 wt%-Li<sup>+</sup>-chitosan film.**

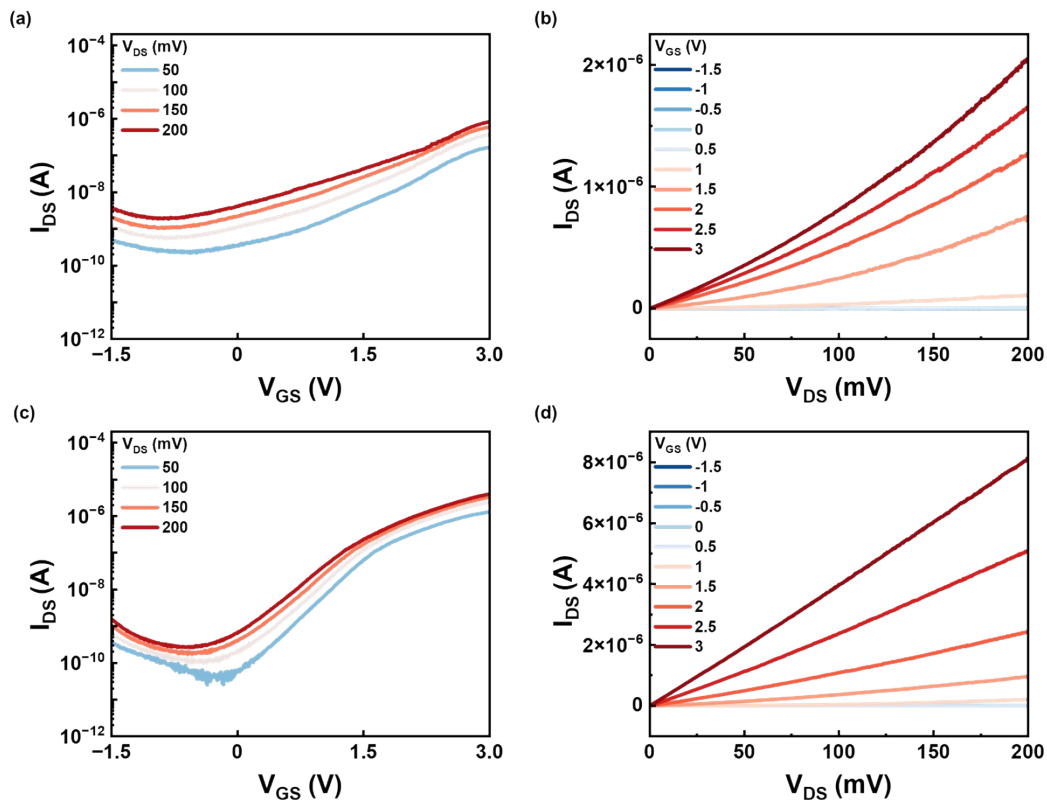
(a) Wide-scan XPS spectrum of the sample, with characteristic peaks of Li, C, N, and O labeled. (b) High-resolution XPS spectrum of the Li 1s region. The low Li concentration results in weak signals. Two peaks are identified at binding energies of 55.45 eV and 57.98 eV, corresponding to ionized Li<sup>+</sup> and LiClO<sub>4</sub>, respectively.



**Supplementary Figure S2. Experimental impedance diagrams of solid electrolyte films: (a) Chitosan (b) 1 wt% Li<sup>+</sup>-chitosan, and (c) 5 wt% Li<sup>+</sup>-chitosan.**

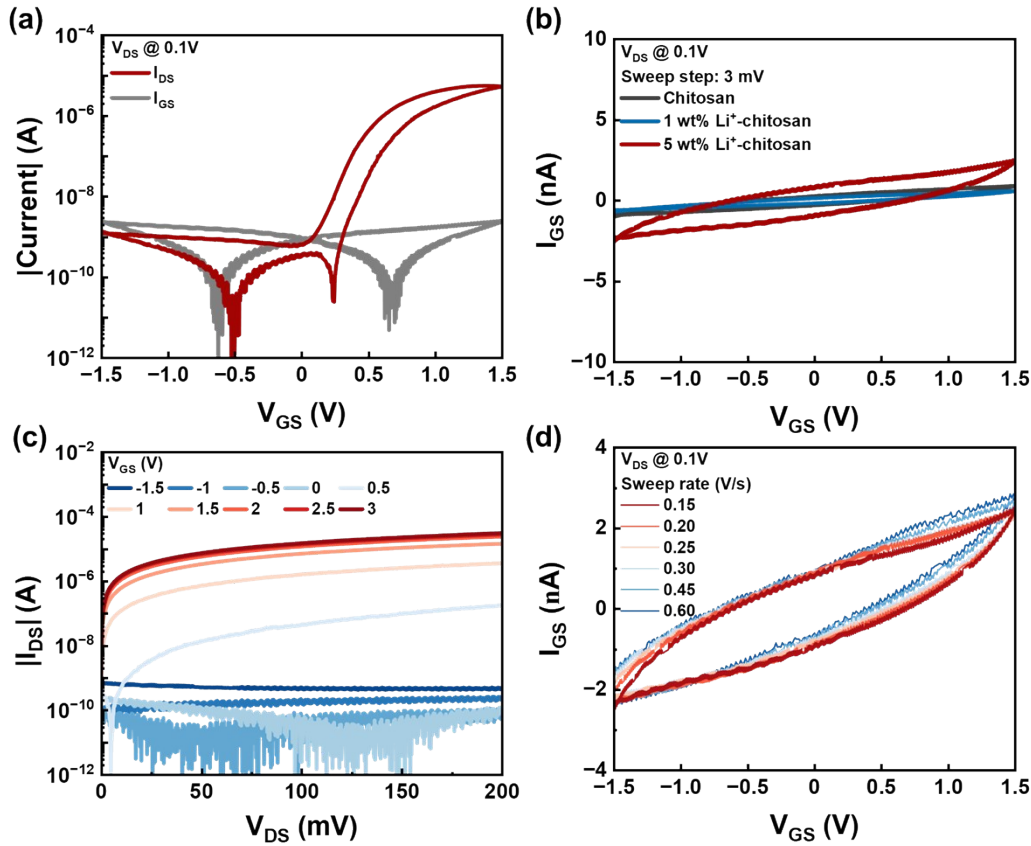
Each panel displays the impedance spectrum ( $Z_I$  vs.  $Z_R$ ) obtained simultaneously with the frequency-dependent specific capacitance measurements in Figure 2b. The high-frequency region (left part of the curve) is fitted with a semicircle to estimate the bulk resistance ( $R_b$ ) of the electrolytes [Scientific Reports, 6, 23578 (2016); Physica B, 405, 4439 (2010)], with the obtained  $R_b$  values labeled. The ionic conductivity  $\sigma$  is calculated using:  $\sigma = L/[A(R_b - R_0)]$ , where  $L$  is the thickness of the electrolyte

dielectric layer,  $A$  is the electrode area, and  $R_0$  represents the inherent impedance of the measurement system. The ionic conductivities are determined to be  $3.3 \times 10^{-6}$  S/cm (Chitosan),  $2.8 \times 10^{-6}$  S/cm (1 wt% Li<sup>+</sup>-chitosan), and  $1.3 \times 10^{-4}$  S/cm (5 wt% Li<sup>+</sup>-chitosan) respectively, indicating significant enhancement with higher Li<sup>+</sup> incorporation.



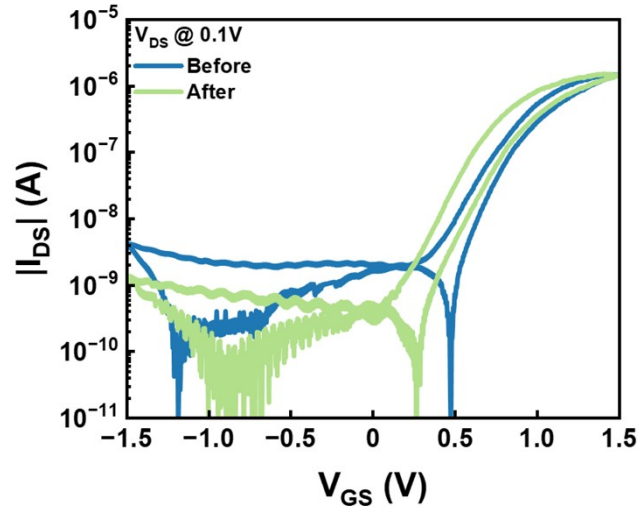
**Supplementary Figure S3. Output and transfer characteristics of chitosan and 1 wt%-Li<sup>+</sup>-chitosan EDL-Ts.**

(a, b) Output and transfer characteristics of the chitosan-based EDL-T. (c, d) Output and transfer characteristics of the 1 wt%-Li<sup>+</sup>-chitosan EDL-T.



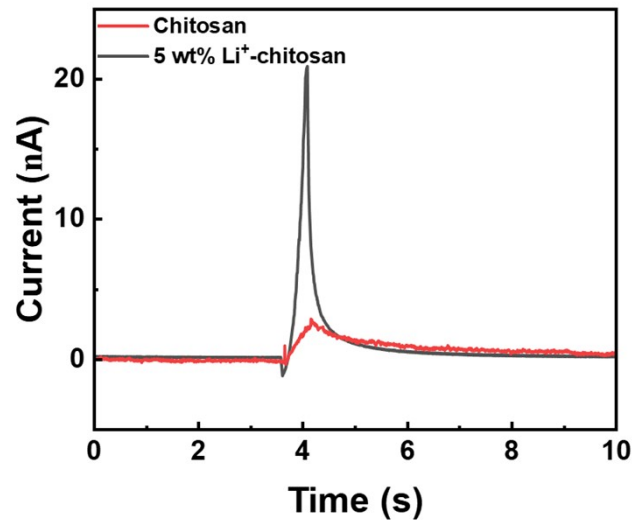
**Supplementary Figure S4. Gate leakage current characterization.**

(a) Gate leakage current ( $I_{GS}$ ) and source-drain current ( $I_{DS}$ ) during the hysteresis measurement of the 5 wt%  $\text{Li}^+$ -Chitosan EDL-T, as shown in Figure 2e. The  $I_{DS}$  exhibits behavior consistent with  $I_{GS}$  when the channel is off, indicating that the  $I_{DS}$  at negative  $V_{GS}$  is primarily due to gate leakage current. (b) Gate leakage current measured simultaneously with the hysteresis curves in Figure 2e. The leakage is significantly higher for the 5 wt%  $\text{Li}^+$ -Chitosan EDL-T due to enhanced ionic conductivity from  $\text{Li}^+$  incorporation. (c) Log-scale output characteristics of the 5 wt%  $\text{Li}^+$ -Chitosan EDL-T, showing low and  $V_{DS}$ -independent  $I_{DS}$  at around  $V_{GS} = 0$  V, confirming that the channel is effectively turned off. (d) Gate leakage current measured simultaneously with the hysteresis curves in Figure 2f at different sweep rates, exhibiting a loop feature and remaining relatively stable across sweep rates.



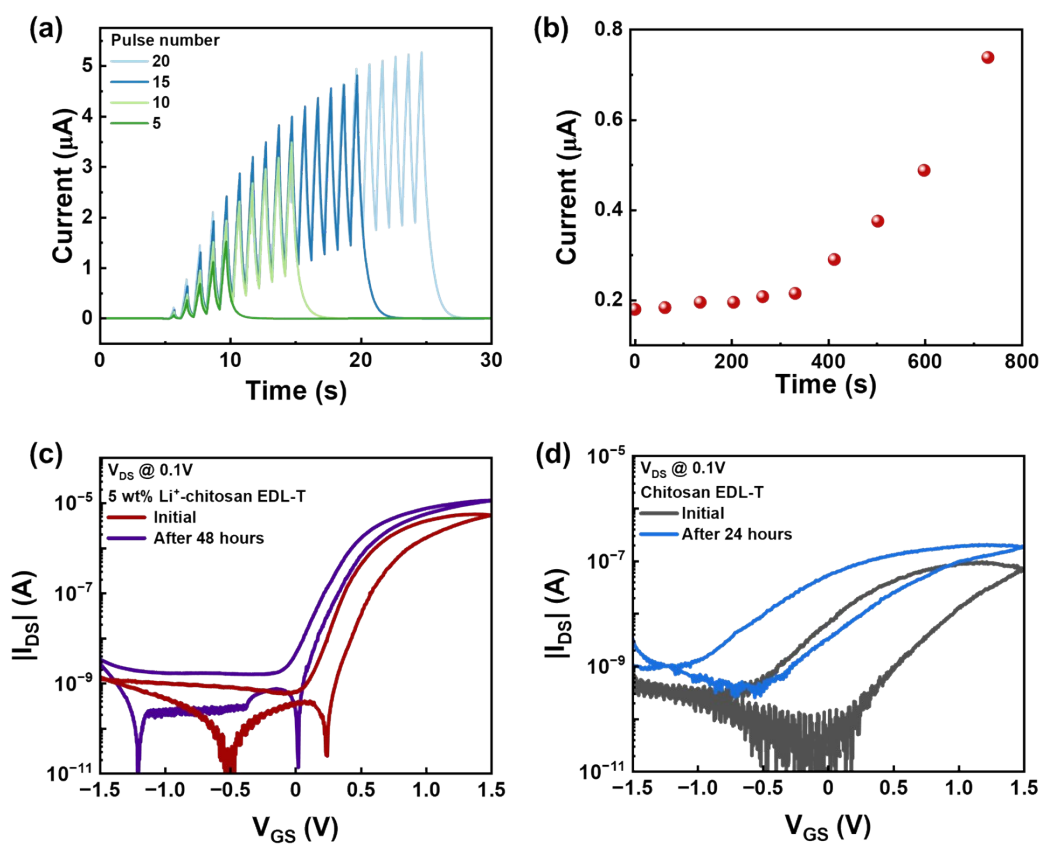
**Supplementary Figure S5. Electrical stability of the 5 wt%-Li<sup>+</sup>-chitosan EDL-T before and after electrolyte cleaning.**

To verify device reliability upon the electrolyte cleaning process, the electrolyte on the original 5 wt%-Li<sup>+</sup>-chitosan EDL-T (“before”) was dissolved using 10 wt% acetic acid and re-coated with the same electrolyte, forming a second 5 wt%-Li<sup>+</sup>-chitosan EDL-T (“after”). The bidirectional transfer characteristics ( $V_{GS}$ :  $-1.5$  V to  $+1.5$  V and back to  $-1.5$  V,  $V_{DS} = 0.1$  V, sweep rate:  $0.15$  V/s) show that the on-state current and hysteresis window remain nearly unchanged, confirming that the cleaning process does not significantly affect device performance.



**Supplementary Figure S6. Comparison of synaptic responses between a chitosan EDL-T and a 5 wt%-Li<sup>+</sup>-chitosan EDL-T.**

Postsynaptic current induced by a single-spike pulse (2 V, 500 ms) is shown for both devices. The 5 wt%-Li<sup>+</sup>-chitosan EDL-T exhibits a significantly higher EPSC peak than the chitosan EDL-T under the same pulse stimulation. However, the EPSC in the Li<sup>+</sup>-incorporated device decays more rapidly, as evident by its higher EPSC after  $t = 5$  s, indicating faster ionic dynamics.



**Supplementary Figure S7. Stability test of 5 wt% Li<sup>+</sup>-Chitosan EDL-T and Chitosan EDL-T devices.**

(a) Overlay of EPSC data from Figure 3c for 5 wt% Li<sup>+</sup>-Chitosan EDL-T, showing  $I_{DS}$  curves of four sequential groups (5, 10, 15, and 20 pulses, 120 s intervals). The first 5 pulses in later measurement groups exhibit higher EPSC peaks, though the  $I_{DS}$  after each group fully relaxes to its initial value. (b) Peak current of single pulses ( $V_{GS} = 2$  V, 500 ms duration, 50–130 s intervals) on 5 wt% Li<sup>+</sup>-Chitosan EDL-T as a function of time, showing a gradual increase in later pulses. The trends in (a) and (b) may indicate long-term potentiation shifting the channel toward its on-state or electrolyte instability due to moisture adsorption. (c, d) Hysteresis characteristics of 5 wt% Li<sup>+</sup>-Chitosan EDL-T (c) and Chitosan EDL-T (d), measured for as-prepared devices and after 1–2 days of ambient air exposure. After prolonged exposure, both devices exhibit increased current, a leftward shift in  $V_{TH}$ , and a reduced hysteresis window, likely due to moisture adsorption enhancing ion migration. Despite these changes, the 5 wt% Li<sup>+</sup>-Chitosan EDL-T retains enhanced ion mobility compared to the Chitosan EDL-T, indicating the robustness of Li<sup>+</sup> doping.